

This paper is part of the Special Issue on [Design and Manufacturing in Biomedical Engineering](#).

**Guest Editor:** Dr. Jashanpreet Singh, University Center for Research and Development, Chandigarh University, Punjab, India.  
Prof. Dr. Chander Prakash, University Center for Research and Development, Chandigarh University, Punjab, India.

Received October 28, 2025, accepted January 28, 2026, publication date for online-first March 17, 2026.

## Original Research Article

# Adhesion Characteristics of HAp Functional Coatings onto 3D-Printed Ti-6Al-4V and PEEK IPCs for Enhanced Bioactivity

Sahil Mehta<sup>1,\*</sup>, Abhineet Saini<sup>2</sup>

<sup>1</sup>Chitkara University Research and Innovation Network, Chitkara University, Rajpura, Punjab, India.

<sup>2</sup>Department of Mechatronics Engineering, Chitkara University, Rajpura, Punjab, India.

\*Corresponding Author Email: [sahil.mehta@chitkara.edu.in](mailto:sahil.mehta@chitkara.edu.in)

### ABSTRACT

The current study probes the growth and characterization of composite hydroxyapatite (HAp) coatings on titanium alloy (Ti-6Al-4V, Grade 5 titanium) + polyetheretherketone (PEEK) substrates by a biomimetic deposition technique. HAp coatings were deposited on three titanium-based substrates: solid Ti-6Al-4V, three-dimensional printed porous Ti-6Al-4V, and interpenetrating composites (IPCs) Ti-6Al-4V + PEEK utilizing 10× concentrated simulated body fluid (SBF) buffered in tris (hydroxymethyl) aminomethane (TRIS or tromethamine) solution at physiological temperature (37 °C). Analysis of adhesion strength was carried out for assessing the mechanical bonding behavior of HAp coating with various substrate configurations. Surface analysis methods, such as scanning electron microscopy and energy dispersive spectrometry, established the growth of crystalline HAp with morphology similar to bone with all substrates. The findings proved that porous Ti-6Al-4V substrates had better adhesion strength through increased mechanical interlocking, and composite Ti-6Al-4V + PEEK substrates had a better stress distribution and a lower interface mismatch. The values of adhesion strength were from  $16.6 \pm 2.0$  megapascal (MPa) for non-treated coatings to  $30.0 \pm 2.0$  MPa for optimized composite coatings, greatly surpassing the minimum clinical requirements of  $\geq 10$  MPa. The displaced biomimetic HAp coatings enhanced wettability, better corrosion resistance, and increased apatite formation in SBF, relative to uncoated substrates. These results indicate that composite HAp coatings on Ti-6Al-4V + PEEK IPCs are a potential method for fabricating superior bioactive implant surfaces with outstanding mechanical and biological performance for orthopedic and dental applications.

**Keywords**—*Biomedical implants, HAp coating, PEEK, Ti-6Al-4V, Biomimetic deposition, Osteointegration.*

**Copyright © 2026.** This is an open-access article distributed under the terms of the Creative Commons Attribution License (CC BY): [Creative Commons - Attribution 4.0 International - CC BY 4.0](#). The use, distribution or reproduction in other forums is permitted, provided the original author(s) and the copyright owner(s) are credited and that the original publication in this journal is cited, in accordance with accepted academic practice. No use, distribution or reproduction is permitted which does not comply with these terms.

## INTRODUCTION

Titanium alloys, particularly Ti-6Al-4V (Grade 5 titanium), are the gold standard for medical implants because of their excellent mechanical properties, corrosion resistance, and biocompatibility. However, in spite of these favorable characteristics, Ti-6Al-4V suffers from inherent biological inertness and susceptibility to stress shielding effect, both of which are detrimental to long-term implant success and osseointegration.<sup>1,2</sup> The moduli mismatch between titanium alloys (110 gigapascal [GPa]) and natural bone (15–30 GPa) have a tendency to lead to stress concentration and consequent bone resorption at sites of implants.<sup>3–5</sup> To overcome these drawbacks, researchers have tried to investigate numerous surface modification techniques, with composite hydroxyapatite (HAp) coating being a highly promising method. Hydroxyapatite,  $\text{Ca}_{10}(\text{PO}_4)_6(\text{OH})_2$ , the principal mineral component of natural human bone, is a highly osteoconductive and biocompatible material that can be an ideal candidate for enhancing the bioactivity of the implant.<sup>6–8</sup> HAp coatings can potentially significantly improve the bone–implant integration by providing a bioactive surface for rapid osseointegration and reduced healing time.

The latest advances in biomaterials have encountered the creation of composite systems where titanium alloys are mixed with polyetheretherketone (PEEK), a high-performance thermoplastic that is popularly known due to its desirable properties. PEEK has a number of positive characteristics, such as excellent chemical resistance, radiolucidity, and an elastic modulus (3.5–4 GPa) that is nearly identical to that of cortical bone, thus reducing the stress-shielding effect. PEEK is used with Ti-6Al-4V to create composite structures that form an attractive pool of mechanical strength and elasticity with native bone tissue.<sup>9–11</sup> Conventional approaches to the deposition of HAp surface, such as sol–gel processing, plasma spraying, and electrophoretic deposition, generally result in crystalline pores with poor adhesion and constrained biological functionality. As an alternative, biomimetic deposition has the advantage of mimicking the process of bone mineralization in nature. In this test, substrates are put into super-saturated simulated body fluid (SBF), which is similar to the ionic composition of human plasma and favors the growth of bone like apatite with enhanced

biological functionality.<sup>12</sup> In order to speed up coating formation at physiological conditions,  $5\times$ – $10\times$  concentrated solutions of SBF are usually used, whereas tris (hydroxymethyl) aminomethane (TRIS or tromethamine) buffer is necessary to keep a constant pH of approximately 7.4 during the coating process. Consequently, nanoscale morphology carbonated HAp, similar to natural bone mineral, is obtained, with greater bioactivity than synthetic HAp coatings.<sup>13–16</sup>

Some of the most important parameters that define the long-term success of coated implants include the adhesion strength between titanium substrate and HAp layer. Lack of proper adhesiveness can lead to delamination of coating and ultimate failure of implant. Crystallinity, coating thickness, surface pretreatment, and interfacial chemistry are some of the factors that are decisive in defining adhesion. It is thus critical to investigate these mechanisms in a variety of substrate geometries, such as solid Ti-6Al-4V, porous three-dimensional (3D)-printed Ti-6Al-4V, and Ti-6Al-4V + PEEK interpenetrating composites (IPCs), to optimize coating performance and clinical applicability.<sup>17–19</sup>

Titanium porous architectures are especially investigated due to their capability to strengthen bone growth as well as to reduce stress shielding. The networks of their pores are interconnected, which enhances surface area, hence resulting in mechanical interlocking and greater adhesion of HAp. Complicated geometries of porous structures are however a challenge in the uniformity of coating deposition as well as in a consistent quantification of adhesion strength.<sup>20,21</sup> Although titanium implants have been extensively studied with respect to HAp coatings, there is still a lack of data on the behavior of biomimetic HAp coatings on Ti-6Al-4V + PEEK IPCs, there is a dearth of data on the behavior of biomimetic HAp coverings on Ti-6Al-4V + PEEK IPCs. The interfacial relationships between the layers of HAp and PEEK composites have been poorly studied, particularly in relation to the effect of polymer phase on adhesion and mechanical stability. The current work fills these gaps in knowledge by conducting systematic research, exploring biomimetic HAp coatings on three substrate materials, such as bulk Ti-6Al-4V, porous Ti-6Al-4V and Ti-6Al-4V + PEEK composites. With the help of SBF  $10\times$  buffered with TRIS, the paper aims

at streamlining the coating procedure and conducting in-depth characterization of coating structure, composition, and adhesion strength.<sup>22-24</sup> These results are probably to provide important understanding of how to develop next-generation bioactive implant surface with improved mechanical reliability and biological integration to be used in clinical practice.

## MATERIALS AND METHODOLOGY

The quality of HAp coatings onto pure Ti-6Al-4V alloy was compared to that on 3D-printed porous Ti-6Al-4V alloy and Ti-6Al-4V + PEEK composite. This section presents the material configuration of various substrates along with HAp coating preparation.

### Sample Fabrication

Ti-6Al-4V alloy (99.5% purity) annealed round bar was purchased and cut to three substrates of varying configurations: solid Ti-6Al-4V discs (10-mm diameter × 5-mm thickness). Selective laser melting (SLM) technique, additive manufacturing technique, was used to fabricate porous Ti-6Al-4V scaffolds, in which a high-energy laser selectively melts successive layers of Ti-6Al-4V powder to fabricate fully dense, near-net shape components. The process enables precise control over microstructure, mechanical properties, and complex geometries. A porous Ti-6Al-4V scaffold with 65% porosity and 200–400-μm pore size, and composite 3D printed Ti-6Al-4V + PEEK samples, was fabricated by injection moulding of PEEK into Ti-6Al-4V scaffolds. All substrates were successively polished using silicon carbide (SiC) papers (400–1,200 grit size) and subsequently cleaned in acetone, distilled water, and ethanol for 10 min.

### Solution Preparation

#### TRIS Buffer Solution Preparation

Chemicals of analytical grade (99.9% purity) used to prepare solutions were as follows: sodium chloride (NaCl), calcium chloride dihydrate (CaCl<sub>2</sub>·2H<sub>2</sub>O), potassium

chloride (KCl), sodium hydrogen phosphate (Na<sub>2</sub>HPO<sub>4</sub>), sodium hydrogen carbonate (NaHCO<sub>3</sub>), magnesium chloride hexahydrate (MgCl<sub>2</sub>·6H<sub>2</sub>O), and TRIS (Sigma-Aldrich, St. Louis, MO, USA). A solution of 2 mg (mL)<sup>-1</sup> dopamine hydrochloride (Sigma-Aldrich), in 10-mM TRIS buffer at pH 8.5, was used to create a thin layer of polydopamine (PDA). The PDA layer served solely as an adhesion-promoting interfacial layer to facilitate uniform HAp deposition. TRIS buffer was prepared in laboratory by dissolving 1.21 g Trizma® base (Loba-Chemie Pvt. Ltd., Mumbai, India) in deionized water, and diluted to 1-L final volume. The pH was set at 7.4 by a gradual addition of about 6–7 mL of concentrated HCl, cooling the solution prior to final pH reading, and any further adjustments.<sup>25-28</sup>

#### Preparation of 10× SBF Solution

In laboratory, 10× SBF solution was prepared according to the chemical composition listed in Table 1. All chemicals used were obtained from Loba-Chemie. Therefore, to make 2 L of SBF solution, chemicals were added sequentially to 1,000 mL of deionized water. An 800-rpm constant-speed magnetic stirrer was used to stir chemicals until they were dissolved. More deionized water was added to make a total volume of 2 L, and the pH was set at 7.4 by slow addition of NaHCO<sub>3</sub>.<sup>29,30</sup>

TABLE 1. Composition of chemicals used to prepare 10× SBF solution.

S. No.	Chemical	Formula	Amount (g)	Concentration (mM)
1.	Sodium chloride	NaCl	115.76	10 <sup>3</sup>
2.	Potassium chloride	KCl	0.7456	5 <sup>1</sup>
3.	Calcium chloride dihydrate	CaCl <sub>2</sub> (2H <sub>2</sub> O)	6.3508	5 <sup>2</sup>
4.	Magnesium chloride hexahydrate	MgCl <sub>2</sub> (6H <sub>2</sub> O)	4.0330	5 <sup>1</sup>
5.	Sodium dihydrogen phosphate	(NaH <sub>2</sub> PO <sub>4</sub> )	2.3996	10

All Ti-6Al-4V substrates were pretreated in alkaline conditions to enhance surface reactivity toward biomimetic coating. The samples were immersed in 5 M NaOH solution at 50 °C for 24 h, rinsed thoroughly with water, and air-dried at 40 °C. The treatment introduces surface hydroxyl moieties that serve as nucleation regions for HAp crystallization. In the case of Ti-6Al-4V porous samples, the alkaline treatment was performed in vacuum to ensure complete infiltration of NaOH solution within pore structure. Pretreated composite Ti-6Al-4V + PEEK IPCs were subjected to modified conditions with 2 M NaOH for 40 °C for 12 h to prevent PEEK degradation.

### Biomimetic Coating Process

Biomimetic HAp coating was performed through 10× SBF immersion process. Pretreated substrates were placed in a freshly prepared 10× SBF solution (TRIS-buffered to pH 7.4) at 37 °C ± 1 °C in a temperature-controlled incubator. The solution was slowly agitated at 70 rpm by an orbital shaker for even distribution of ions. The coating process continued for 7 days for a solution–substrate volume ratio of 100:1 to prevent depletion with daily solution renewal during the first 3 days and then at every 48 hs. Samples were taken out gently and cleaned in distilled water after coating and air-dried at 27 °C.

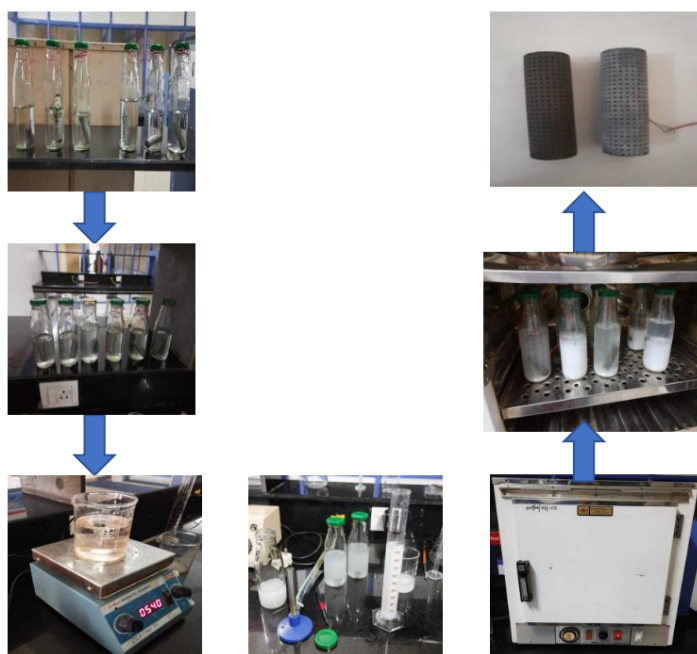


FIGURE 1. Biomimetic coating process.

## RESULTS AND DISCUSSION

### Morphological and Structural Characterization of Coatings

Surface topography of HAp coatings of three different substrate configurations’ was determined by scanning electron microscopy (SEM), and elemental analysis was verified using energy dispersive spectrometry (EDS).

As reflected in the representative SEM micrographs in Figure 2, dense and homogeneous coating was actually deposited on all substrates following immersion in 10× SBF solution for 24 h. On solid Ti-6Al-4V substrate (Figure 2a), the coating consisted of rounded discrete crystallites that had aggregated to form a continuous “cauliflower-like” morphology. This type of morphology is a characteristic of biomimetically precipitated apatite and is said to be favorable for cell adhesion and proliferation.

In case of porous Ti-6Al-4V substrate (Figure 2b), not only was the outer surface covered by HAp coating but it penetrated deeply into the porous structure, encapsulating internal struts. This complete infiltration is critical for inducing bone growth throughout the scaffold. Morphology within pores was equal, compared to that on the solid surface.

The coating formed on Ti-6Al-4V + PEEK composite substrate (Figure 2c) was checked to cover both titanium and polymeric areas and was equal, which indicated that alkaline pretreatment successfully conditioned the surfaces to enable the growth of apatite. The interface between coated and uncoated regions was found to be continuous and did not appear to have any apparent discontinuity, and this demonstrated high levels of interfacial integration.

Energy-dispersive spectroscopy of a typical coated specimen (Figure 2d) showed that the coating was mostly composed of calcium (Ca) and phosphorus (P). The final Ca–P atomic ratio was about 1.65, which was quite near the stoichiometric ratio of 1.67 of crystalline HAp ( $\text{Ca}_{10}(\text{PO}_4)_6(\text{OH})_2$ ). Besides, traces of magnesium (Mg) and sodium (Na) were also discovered. Their occurrence was due to the incorporation of SBF ions, which usually replaces into apatite lattice, creating a carbonated HAp that is much more similar to the mineral composition of the bone of natural origin.

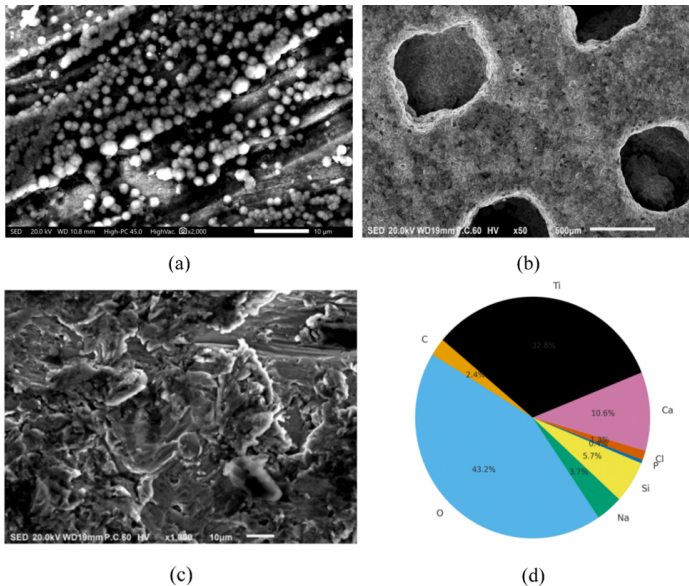


**FIGURE 2.** (a) SEM image of HAp coating on solid Ti-6Al-4V. (b) SEM image of HAp coating on porous Ti-6Al-4V. (c) SEM image of HAp coating on Ti-6Al-4V + PEEK IPC. (d) Representative EDS spectrum of HAp coating.

The elemental composition of HAp coatings formed on different samples is listed in Table 2. The coating trend demonstrated that thickness was comparatively more in porous and composite samples, compared to traditional solid samples.

The calculated Ca-P atomic ratios were approximately 2.35, 1.64, and 1.62 for 12, 24, and 48 h of immersion, respectively. The Ca-P ratios for 24 and 48 h were close to the stoichiometric value of HAp (1.67), suggesting improved apatite formation and maturation with longer duration of immersion. These results confirmed the successful formation of a calcium phosphate ( $\text{Ca}_3(\text{PO}_4)_2$ )-rich HAp coating on substrate surface as shown in Table 3.

**TABLE 2.** Mass and thickness of HAp coating on different samples.

Sample	Initial Mass (mg)	Final Mass (mg)	Mass Gained (mg)	Coating Thickness ( $\mu\text{m}$ )
HAp (solid Ti6Al4V)	3,779.4	3,838.8	59.4	39.78
HAp (porous Ti6Al4V)	2,718.6	2,816.3	97.7	65.32
HAp (Ti6Al4V + PEEK)	2,730.2	2,832.8	102.6	54.16

**TABLE 3.** HAp coating constituents using EDS technique for Ca-P ratios.

Elements	HAp (12 h)		HAp (24 h)		HAp (48 h)	
	Wt%	At%	Wt%	At%	Wt%	At%
Ti	59.83	37.38	37.89	22.69	36.22	20.62
O	27.97	52.32	43.62	64.77	44.94	66.79
Ca	7.88	5.89	10.55	6.39	10.84	6.51
P	2.61	2.51	5.35	3.89	5.58	4.01
Al	1.71	1.9	2.59	2.26	2.42	2.07
Total	100	100	100	100	100	100
Ca-P ratio		2.35		1.64		1.62

### Coating Adhesion Strength

The mechanical integrity of biomimetic HAp coatings was quantitatively assessed using pull-off adhesion and scratch tests. The results, summarized in Figure 3, revealed significant differences in adhesion strength among the three substrate configurations.

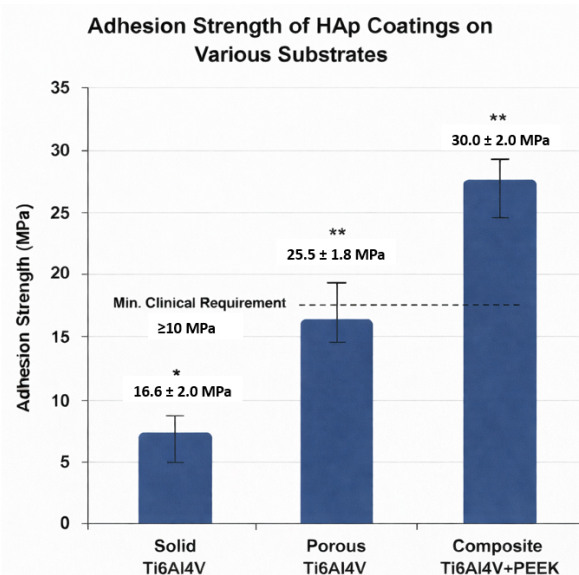


**FIGURE 3.** Adhesion strength comparison graph (\* $p < 0.05$ ; \*\* $p < 0.01$ ).

The pull-off test revealed that the solid Ti-6Al-4V substrate had the lowest adhesion strength of  $16.6 \pm 2.0$  megapascal (MPa). The porous Ti-6Al-4V scaffolds had a remarkable improvement, with an adhesion strength of  $25.4 \pm 1.8$  MPa. The maximum adhesion value was for the

Ti-6Al-4V + PEEK IPC, which had an adhesion strength of  $30.0 \pm 2.0$  MPa. Its graphical illustration is shown in Figure 3.

The scratch tests were performed according to ASTM C1624-05 using a Rockwell diamond indenter (200- $\mu$ m tip), with a load range of 0–80 N, a loading rate of 10 N  $\text{min}^{-1}$ , and a scratch speed of 10 mm  $\text{min}^{-1}$ . The results of scratch tests confirmed the trends of pull-off tests. The dense Ti-6Al-4V coatings fractured at the lowest critical loads, with the initial cohesive cracks ( $L_{c1}$ ) at  $18.5 \pm 1.2$  N and a full coating delamination ( $L_{c2}$ ) at  $35.2 \pm 2.5$  N. The porous and composite substrates showed increasingly higher critical loads. The highest scratch resistance was shown by Ti-6Al-4V + PEEK IPC with  $L_{c1}$  and  $L_{c2}$  at  $32.4 \pm 2.1$  N and  $55.1 \pm 2.8$  N, respectively. These results are shown in Figure 4.

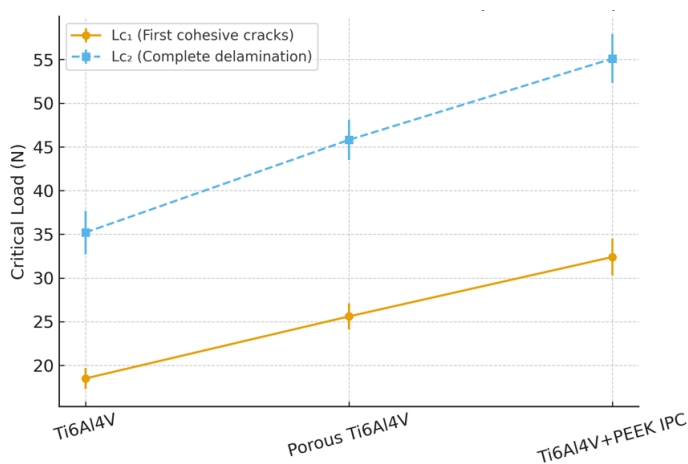


FIGURE 4. Graph showing scratch test results.

### CONCLUSION

This research effectively illustrates the biomimetic deposition of a crystalline, uniform, and bone-like HAp coating onto solid Ti-6Al-4V, porous Ti-6Al-4V, and new Ti-6Al-4V + PEEK composite substrates.

The findings clearly indicate that substrate architecture significantly influences the coating’s mechanical performance. The highest adhesion strength was shown by Ti-6Al-4V + PEEK composite, which exceeded both porous and solid Ti-6Al-4V in a significant manner. This higher performance was due to lower elastic modulus of the PEEK component, which reduces stress at the coating–substrate interface. In addition, porosity increased

adhesion by mechanical interlocking. All coated substrates considerably exceeded the minimum requirements of clinical adhesion strength, establishing their mechanical stability. Finally, HAp-coated Ti-6Al-4V + PEEK IPCs are very promising material for next-generation dental and orthopedic implants, with an ideal blend of bioactivity and improved mechanical stability.

### AUTHOR CONTRIBUTIONS

Conceptualization, S.M. and A.S.; Methodology, S.M. and A.S.; Software, S.M.; Hardware, S.M., Validation, S.M.; Formal Analysis, S.M.; Investigation, S.M. and A.S.; Writing–Original Draft Preparation, S.M.; Writing–Review & Editing, S.M. and A.S.; Visualization, S.M. and A.S.; Supervision, A.S.

### ACKNOWLEDGEMENTS

Not applicable.

### FUNDING

This research received no external funding.

### DATA AVAILABILITY STATEMENT

Not applicable.

### CONFLICT OF INTEREST

The authors declared no conflict of interest.

### ETHICS APPROVAL AND CONSENT TO PARTICIPATE

Not applicable.

### CONSENT FOR PUBLICATION

Not applicable.

### FURTHER DISCLOSURE

Not applicable.

### REFERENCES

1. Kokubo, T, Takadama, H. How useful is SBF in predicting in vivo bone bioactivity? *Biomaterials*. 2006;27(15):2907–2915. <https://doi.org/10.1016/j.biomaterials.2006.01.017>.

2. Hench, L.L. Bioceramics: from concept to clinic. *J Am Ceramic Soc.* 1991;74(7):1487–1510. <https://doi.org/10.1111/j.1151-2916.1991.tb07132.x>.
3. LeGeros, R.Z. Calcium Phosphates in Oral Biology and Medicine. In *Monographs in Oral Science*. Lussi, A., Buzalaf, M.A.R., eds. S. Karger AG: Basel, Switzerland; 1991; Vol. 15, pp. 201. <https://doi.org/10.1159/000419232>.
4. Kurtz, S.M., Devine, J.N. PEEK biomaterials in trauma, orthopedic, and spinal implants. *Biomaterials.* 2007;28(32):4845–4869. <https://doi.org/10.1016/j.biomaterials.2007.07.013>.
5. Wang, M. Developing bioactive composite materials for tissue replacement. *Biomaterials*, 24(13):2133–2151. [https://doi.org/10.1016/S0142-9612\(03\)00037-1](https://doi.org/10.1016/S0142-9612(03)00037-1).
6. de Groot, K., Geesink, R., Klein, C.P., et al. Plasma-sprayed coatings of hydroxylapatite. *J Biomed Mat Res.* 1987;21(12):1375–1381. <https://doi.org/10.1002/jbm.820211203>.
7. Tas, A.C., Bhaduri, S.B. Rapid coating of Ti-6Al-4V at room temperature with a calcium phosphate layer. *J Mater Res.* 2004;19(10):2742–2749. <https://doi.org/10.1557/JMR.2004.0349>.
8. Kim, H.M., Himeno, T., Kawashita, M., et al. The mechanism of biomineralization of bone-like apatite on synthetic hydroxyapatite: an in vitro assessment. *J Royal Soc Interf.* 2004;1(1):17–22. <https://doi.org/10.1098/rsif.2004.0003>.
9. Ryan, G., Pandit, A., Apatsidis, D.P. Fabrication of porous titanium scaffolds for bone tissue engineering. *Int J Biomater.* 2006;30:141. <https://doi.org/10.1016/j.biomaterials.2008.05.032>.
10. Brown, T., Bao, Q.B., Agrawal, C.M., et al. An in vitro assessment of wear particulate generated from NUBAC: a PEEK-on-PEEK articulating nucleus replacement device: methodology and results from a series of wear tests using different motion profiles, test frequencies, and environmental conditions. *Spine.* 2011;36(26):E1675–E1685. <https://doi.org/10.1097/BRS.0b013e31821ac8a0>.
11. Suchanek, W., Yoshimura, M. Processing and properties of hydroxyapatite-based biomaterials for use as hard tissue replacement implants. *J Mater Res.* 1998;13(1):94–117. <https://doi.org/10.1557/JMR.1998.0015>.
12. Liu, X., Chu, P.K., Ding, C. Surface modification of titanium, titanium alloys, and related materials for biomedical applications. *Mater Sci Eng R Rep.* 2004;47(3–4):49–121. <https://doi.org/10.1016/j.mser.2004.11.001>.
13. Barrere, F., van der Valk, C.M., Dalmeijer, R.A., et al. Osteogenicity of biomimetic apatite coating applied on metal implants. *Biomaterials.* 2003;24(4):531–538. <https://doi.org/10.1002/jbm.a.10454>.
14. Webster, T.J., Ergun, C., Doremus, R.H., et al. Specific proteins mediate enhanced osteoblast adhesion on nanophase ceramics. *J Biomed Mater Res.* 2000;51(3):475–483. [https://doi.org/10.1002/1097-4636\(20000905\)51:3<475::AID-JBM23>3.0.CO;2-9](https://doi.org/10.1002/1097-4636(20000905)51:3<475::AID-JBM23>3.0.CO;2-9).
15. Ozhukil Kollath, V., Chen, Q., Mullens, S., et al. Electrophoretic deposition of hydroxyapatite and hydroxyapatite-alginate on rapid prototyped 3D Ti-6Al-4V scaffolds. *J Mater Sci.* 2016;51(5):2338–2346. <https://doi.org/10.1007/s10853-015-9543-6>.
16. Geesink, R.G.T., de Groot, K., Klein, C.P.A.T. Bonding of bone to apatite-coated implants. *J Bone Joint Surg Br Vol.* 1988;70(1):17–22. <https://doi.org/10.1302/0301-620X.70B1.2828374>.
17. Yin, C., Zhang, T., Wei, Q., et al. Surface treatment of 3D printed porous Ti-6Al-4V implants by ultraviolet photofunctionalization for improved osseointegration. *Bioact Mater.* 2022;7:26–38. <https://doi.org/10.1016/j.bioactmat.2021.05.043>.
18. Oyane, A., Kim, H.M., Furuya, T., et al. Preparation and assessment of bioactivity of a bone-like apatite/poly(lactic acid) composite. *J Biomed Mater Res A.* 2003;64(2):339–346. <https://doi.org/10.1002/jbm.a.10426>.
19. Balla, V.K., Bodhak, S., Bose, S., et al. Porous tantalum structures for bone implants: fabrication, mechanical and in vitro biological properties. *Acta Biomater.* 2010;6(8):3349–3359. <https://doi.org/10.1016/j.actbio.2010.01.046>.
20. Albayrak, O., El-Atwani, O., Altintas, S. Hydroxyapatite coating on titanium substrate by electrophoretic deposition method: effects of titanium dioxide inner layer on adhesion strength and hydroxyapatite decomposition. *Surf Coat Technol.* 2008;202(11):2482–2487. <https://doi.org/10.1016/j.surfcoat.2007.09.031>.
21. Bigi, A., Falini, G., Foresti, E., et al. Magnesium influence on hydroxyapatite crystallization. *J Inorg Biochem.* 1992;46(4):251–257. [https://doi.org/10.1016/0162-0134\(88\)85004-9](https://doi.org/10.1016/0162-0134(88)85004-9).
22. Li, P., Ohtsuki, C., Kokubo, T., et al. The role of hydrated silica, titania, and alumina in inducing apatite on implants. *J Biomed Mater Res.* 1994;28(1):7–15. <https://doi.org/10.1002/jbm.820280103>.
23. Dorozhkin, S.V. Bioceramics of calcium orthophosphates. *Biomaterials.* 2010;31(7):1465–1485. <https://doi.org/10.1016/j.biomaterials.2009.11.050>.
24. Bell, K.R., Clement, N.D., Jenkins, P.J., et al. A comparison of the use of uncemented hydroxyapatite-coated bipolar and cemented femoral stems in the treatment of femoral neck fractures: a case-control study. *Bone Joint J.* 2014;96(3):299–305. <https://doi.org/10.1302/0301-620X.96B3.32271>

25. Li, S., Chen, R., Xu, W., et al. PEEK-Based Orthopedic Composites and Structures for Orthopedic Repair: A Review. *Polym Compos.* 2025;46(17):15567–15583. <https://doi.org/10.1002/pc.70025>.
26. Zreiqat, H., Valenzuela, S.M., Nissan, B.B., et al. The effect of surface chemistry modification of titanium alloy on signalling pathways in human osteoblasts. *Biomaterials.* 2005;26(36):7579–7586. <https://doi.org/10.1016/j.biomaterials.2005.05.024>.
27. Wennerberg, A., Albrektsson, T. Effects of titanium surface topography on bone integration: a systematic review. *Clin Oral Implants Res.* 2009;20(Suppl 4):172–184. <https://doi.org/10.1111/j.1600-0501.2009.01775.x>.
28. Habraken, W., Habibovic, P., Epple, M., et al. Calcium phosphates in biomedical applications: materials for the future? *Mater Today.* 2016;19(2):69–87. <https://doi.org/10.1016/j.mattod.2015.10.008>.
29. Vallet-Regí, M., González-Calbet, J.M. Calcium phosphates as substitution of bone tissues. *Prog Solid State Chem.* 2004;32(1–2):1–31. <https://doi.org/10.1016/j.progsolidstchem.2004.07.001>.
30. Jarcho, M. Calcium phosphate ceramics as hard tissue prosthetics. *Clin Orthop Relat Res.* 1981;157:259–278. <https://doi.org/10.1097/00003086-198106000-00037>.